An Improved Stator Flux Estimation for Speed Sensorless Stator Flux Orientation Control of Induction Motors

Myoung-Ho Shin, *Student Member, IEEE*, Dong-Seok Hyun, *Senior Member, IEEE*, Soon-Bong Cho, and Song-Yul Choe

***Abstract*—This paper proposes a programmable low pass filter (LPF) to estimate stator flux for speed sensorless stator flux orientation control of induction motors. The programmable LPF is developed to solve the dc drift problem associated with a pure integrator and a LPF. The pole of the programmable LPF is located far from the origin in order to decrease the time constant with the increasing speed. In addition, the programmable LPF has the phase/gain compensator to estimate exactly stator flux in a wide speed range. Consequently, the drift problem is much improved and the stator flux is exactly estimated in the wide speed range. The validity of the proposed programmable LPF is verified by speed sensorless vector control of a 2.2 [kW] three-phase induction motor.**

***Index Terms*—Induction motor, sensorless vector control, stator flux estimator.**

I. Introduction

INDUCTION motors have been used more in the industrial variable speed drive system with the development of the vector control technology. This method requires a speed sensor such as a shaft encoder for speed control. However, a speed sensor cannot be mounted in some cases such as motor drives in a hostile environment and high-speed drives. In addition, it requires careful cabling arrangements with attention to electrical noise. Moreover, it causes to become expensive in the system price and bulky in the motor size. Recently several speed sensorless vector control schemes have been proposed [1]–[10].

The stator flux for speed sensorless vector control is estimated by the integration of back emf. The integration of back emf by pure integrator has the drift and the saturation problems by the initial condition and the dc offset. To solve the problems, the pure integrator should be replaced by a low pass filter (LPF) [2]. When the motor frequency is lower than the cutoff frequency of the LPF, an estimation error will be produced. To estimate exactly stator flux in a wide speed range, the LPF should have a very low cutting frequency. However, there still remains the drift problem due to the very large time constant of the LPF.

Manuscript received August 31, 1998; revised August 25, 1999. Recommended by Associate Editor, M. Arefeen.

M.-H. Shin and D.-S. Hyun are with the Department of Electrical Engineering Hanyang University, Seoul 133-791, Korea.

S.-B. Cho is with the Department. of Electrical Engineering, Doowon Technical College, Ansung, Korea.

S.-Y. Choe is with Hyundai Precision and Ind. Company, Ltd., Yongin, Korea.

Publisher Item Identifier S 0885-8993(00)02336-X.

Some efforts have been made to solve the problem [3]–[6]. A digital filter was proposed to solve the drift problem [3]. In this method, the magnitude of stator flux is estimated by a pure integrator, and the synchronous angle and speed are estimated by a digital filter with the pole farther from the origin. However, the magnitude of stator flux vector estimated by pure integrator is not correct due to the drift and the saturation. In addition, when the motor frequency is lower than the cutoff frequency of the digital filter, an error will be produced in the computation of the synchronous angle.

A programmable cascaded LPF was proposed to solve the drift problem and to estimate exactly stator flux [4], [5]. However, the scheme has a drawback in that when the motor speed is very close to zero, the time constant of the LPF will be very large.

This paper proposes a programmable LPF with the phase/gain compensator to estimate precisely the stator flux in a wide speed range. In addition, the pole of the programmable LPF is located far from the origin in order to decrease the time constant as the speed increases. Consequently, the stator flux is exactly estimated and the drift problem is much improved by the small time constant in a wide speed range. The proposed programmable LPF is applied to speed sensorless stator flux-oriented induction motor drive. The validity of the proposed programmable LPF has been proved by the simulation and experiments.

II. Description of Programmable LPF

The principle of the programmable LPF method of integration can be explained as follows.

In the stationary $\alpha-\beta$ reference frame, the stator flux is given by

$$\lambda_s = \int (v_s - R_s i_s)\, dt \tag{1}$$

where v_s = stator voltage, R_s = stator resistance, and i_s = stator current.

The integration of (1) by pure integrator $(1/s)$ involves the drift and the saturation problems. To solve the problems, the pure integrator is replaced by a LPF. The estimated stator flux by the LPF can be given as

$$\frac{\hat{\lambda}_{sl}}{v_e} = \frac{1}{s+a} \tag{2}$$

where "^" = estimated value, $\hat{\lambda}_{sl}$ = estimated stator flux by LPF, a = pole, and v_e = back emf $(v_s - R_s i_s)$.

The phase lag and the gain of (2) can be given as

$$\phi = -\tan^{-1}\left(\frac{\hat{\omega}_e}{a}\right) \tag{3}$$

$$M = \left|\frac{\hat{\lambda}_{sl}}{v_e}\right| = \frac{1}{\sqrt{\hat{\omega}_e^2 + a^2}} \tag{4}$$

where $\hat{\omega}_e$ = estimated synchronous angular frequency.

Fig. 1 shows the phase lag of $\hat{\lambda}_{sl}$ estimated by the LPF, and the phase lag of $\hat{\lambda}_s$ estimated by the pure integrator. The phase lag of $\hat{\lambda}_s$ is 90° and the gain is $1/|\hat{\omega}_e|$. However, the phase lag of the LPF is not 90° and the gain is not $1/|\hat{\omega}_e|$. Consequently, an error will be produced by this effect of the LPF. When the motor frequency is lower than the cutoff frequency of the LPF, the error is more severe. In order to remove this error, the LPF in (2) should have a very low cutting frequency. However, there still remains the drift problem due to the very large time constant of the LPF. For the exact estimation of the stator flux, the phase lag and the gain of $\hat{\lambda}_{sl}$ in (2) have to be 90° and $1/|\hat{\omega}_e|$, respectively. In addition, to solve the drift problem, the pole should be located far from the origin.

In this paper, the decrement in the gain of the LPF is compensated by multiplying a gain compensator, G in (5) and the phase lag is compensated by multiplying a phase compensator, P in (6). The new integrator with the gain and the phase compensator can be given as (7).

$$G = \frac{\sqrt{\hat{\omega}_e^2 + a^2}}{|\hat{\omega}_e|} \tag{5}$$

$$P = \exp(-j\phi_1) \tag{6}$$

$$\frac{\hat{\lambda}_s}{v_e} = \frac{1}{(s+a)} \frac{\sqrt{\hat{\omega}_e^2 + a^2}}{|\hat{\omega}_e|} \exp(-j\phi_1). \tag{7}$$

When the programmable LPF is transformed into the sampled-data model using the difference approximation, the sampled-data model has a modeling error which, in turn, produces an error in the stator flux estimation. This error is more severe when the motor frequency is lower than the cutoff frequency of the LPF. Accordingly, the cutoff frequency can not be located at fixed point far from the origin. If the pole is varied proportionally to the motor speed, the proportion of the motor frequency to the cutoff frequency of the LPF is constant. If the proportion is large, the estimation error will be very small. Consequently, the pole a is determined to be varied proportionally to the motor speed as (8). Therefore, the pole is located close to the origin in very low speed range and far from the origin in high speed range.

$$a = \frac{|\hat{\omega}_e|}{k} \tag{8}$$

where k = constant.

The time constant of the programmable LPF, $k/|\hat{\omega}_e|$, is decreased with the increase of the motor speed.

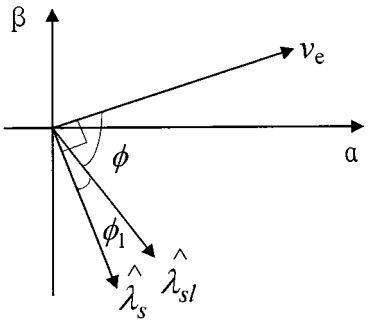

Fig. 1. Vector diagram of LPF and pure integrator.

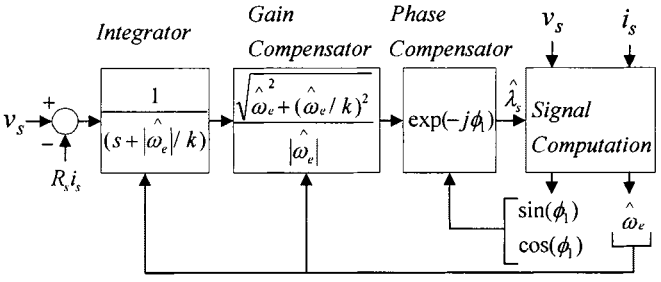

Fig. 2. Block diagram of the programmable LPF.

The complete equation for stator flux estimator can be derived as

$$\frac{\hat{\lambda}_s}{v_e} = \frac{1}{(s+|\hat{\omega}_e|/k)} \frac{\sqrt{\hat{\omega}_e^2 + (\hat{\omega}_e/k)^2}}{|\hat{\omega}_e|} \exp(-j\phi_1) \tag{9}$$

where

$$\exp(-j\phi_1) = \cos(\phi_1) - j\sin(\phi_1)$$

$$\cos(\phi_1) = \frac{|\hat{\omega}_e|}{\sqrt{\hat{\omega}_e^2 + (\hat{\omega}_e/k)^2}}$$

$$\sin(\phi_1) = \frac{\hat{\omega}_e/k}{\sqrt{\hat{\omega}_e^2 + (\hat{\omega}_e/k)^2}}.$$

Fig. 2 shows the block diagram of the programmable LPF.

III. Direct Stator Flux Orientation System

The control scheme of the proposed drive system is speed sensorless stator flux orientation. The stator flux orientation control of induction motor is used more in industrial variable speed drive system because stator flux estimation accuracy is dependent only on the stator resistance variation. In addition, it is insensitive to the variation in the leakage inductance of the machine.

Fig. 3 shows the control block diagram of speed sensorless stator flux orientation control drive that incorporates the proposed programmable LPF. The stator flux magnitude and the transformation angle can be written as follows from the flux in stationary $\alpha - \beta$ reference frame

$$|\hat{\lambda}_s| = \sqrt{\hat{\lambda}_{\alpha s}^2 + \hat{\lambda}_{\beta s}^2} \tag{10}$$

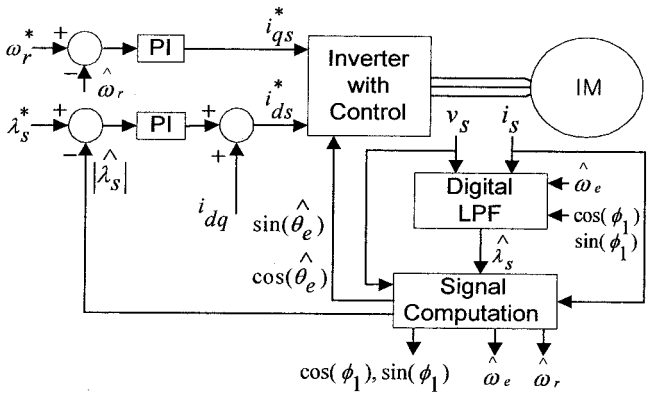

Fig. 3. Block diagram of speed sensorless stator flux orientation control drive.

$$\cos(\hat{\theta}) = \frac{\hat{\lambda}_{\alpha s}}{|\hat{\lambda}_s|} \tag{11}$$

$$\sin(\hat{\theta}) = \frac{\hat{\lambda}_{\beta s}}{|\hat{\lambda}_s|} \tag{12}$$

The estimated slip speed and the decoupling compensation current are represented in rotating d-q reference frame as follows [7].

$$\hat{\omega}_{sl} = \frac{(1+\sigma\tau_r p)L_s i_{qs}}{\tau_r(\lambda_{ds} - \sigma L_s i_{ds})} \tag{13}$$

$$i_{dq} = \frac{\hat{\omega}_{sl}\tau_r\sigma i_{qs}}{(1+\sigma\tau_r p)} \tag{14}$$

where $\sigma = (1 - L_m^2/L_s L_r)$ is the total leakage factor; $\tau_r = L_r/R_r$ is the rotor time constant; L_m is the magnetizing inductance; L_s, L_r is the stator and rotor inductance; and $p = d/dt$ is the differential operator.

The synchronous speed and the rotor speed can be given as

$$\hat{\omega}_e = \frac{((v_{\beta s} - R_s i_{\beta s})\hat{\lambda}_{\alpha s} - (v_{\alpha s} - R_s i_{\alpha s})\hat{\lambda}_{\beta s})}{|\hat{\lambda}_s|^2} \tag{15}$$

$$\hat{\omega}_r = \hat{\omega}_e - \hat{\omega}_{sl} \tag{16}$$

The torque can be written as

$$T_e = \frac{3P_n}{4}\lambda_{ds} i_{qs} \tag{17}$$

where P_n is the number of poles in the machine.

When the slip speed in (13) and decoupling compensation current in (14) are calculated, a differentiator is very sensitive to the noise. The system could be unstable by the noise. To increase the noise immunity of the system, the derivative term is eliminated and steady-state form is used as follows.

$$\hat{\omega}_{sl} = \frac{L_s i_{qs}}{\tau_r(\lambda_{ds} - \sigma L_s i_{ds})} \tag{18}$$

$$i_{dq} = \hat{\omega}_{sl}\tau_r\sigma i_{qs} \tag{19}$$

The control system could be unstable due to the very high peak components included in the slip speed. To make the system stable, a limiter is used to eliminate the very high peak components. The error included in the rotor speed is removed by the use of low pass filter.

TABLE I
INDUCTION MOTOR PARAMETERS.

Parameter		Value
Rated power	2.2	[kW]
Pole number	4	
Magnetizing current(peak)	5	[A]
Rated flux	0.25	[Wb]
Stator resistance	1.26	[Ω]
Rotor resistance	0.2	[Ω]
Magnetizing inductance	50	[mH]
Moment of inertia	0.017	[kg·m^2]
Stator leakage inductance	4.7	[mH]
Rotor leakage inductance	4.7	[mH]

The stator voltage is reconstructed from the inverter switching states. The algorithm of the stator voltage estimation is as follows [10]. A switching function SA for phase A is 1 when upper switch of phase A is on. SA is 0 when lower switch of phase A is on. A similar definition is adopted for phase B and C. The stator phase voltages can be given in terms of switching states and the dc link voltage as follows.

$$v_{as} = \frac{V_{\rm dc}}{3}(2{\rm SA} - {\rm SB} - {\rm SC}) \tag{20a}$$

$$v_{bs} = \frac{V_{\rm dc}}{3}(-{\rm SA} + 2{\rm SB} - {\rm SC}) \tag{20b}$$

$$v_{cs} = \frac{V_{\rm dc}}{3}(-{\rm SA} - {\rm SB} + 2{\rm SC}) \tag{20c}$$

Applying the 3 to 2 phase transformation to (20), stator voltage in stationary $\alpha - \beta$ reference frame can be given as

$$v_{\alpha s} = \frac{V_{\rm dc}}{3}(2{\rm SA} - {\rm SB} - {\rm SC}) \tag{21a}$$

$$v_{\beta s} = \frac{V_{\rm dc}}{\sqrt{3}}({\rm SB} - {\rm SC}) \tag{21b}$$

The processor reads the outputs of prefilter $(s = -2985)$ through an A/D converter. The signal aliasing is prevented by the prefilter. The phase lag and the decrement of gain caused by the prefilter can be neglected because the pole of the prefilter is located so far from the origin.

IV. SIMULATION RESULTS

The proposed programmable LPF was studied by simulation with the drive system shown in Fig. 3. ACSL was used for simulation. The constant k in (9) was determined as 3 for good performance of the drive. The lower limit of a $(=|\hat{\omega}_e|/k)$ is 1 to prevent the time constant of the programmable LPF from being much increased when the motor speed is close to 0 [rpm]. The motor parameters are shown in Table I.

Fig. 4 shows the speed and the flux waveforms by the LPF in (2) with fixed pole $(s = -1)$. Because the pole is close to the origin, the flux and the speed estimation are unstable due to the large time constant of the LPF when the speed is changed from 1500 to 400 [rpm]. Fig. 4(a) shows that the estimated speed is delayed by the use of the LPF. Fig. 4(d) shows that the LPF produces a flux estimation error.

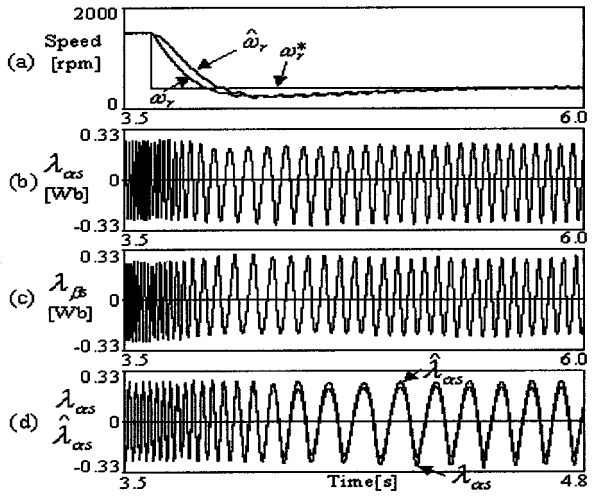

Fig. 4. Step response by LPF with fixed pole $(s = -1)$ (load torque: 6 [N·m], speed reference (ω_r^*): $1500 \rightarrow 400$ [rpm]).

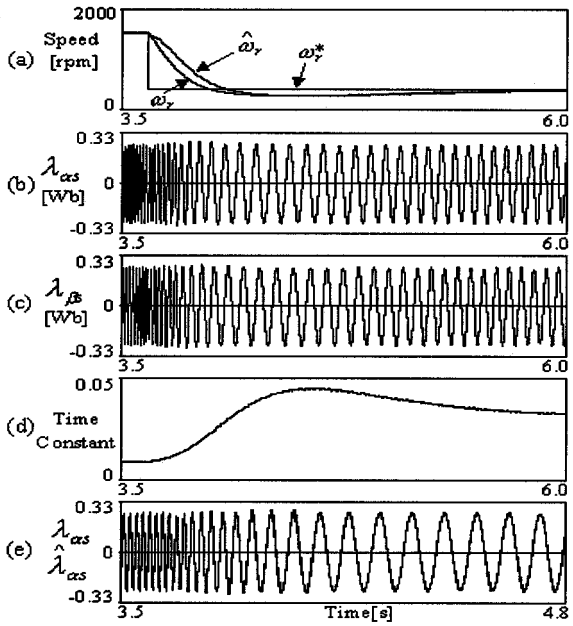

Fig. 5. Step response by programmable LPF (load torque: 6 [N·m], speed reference: 1500 → 400 [rpm]).

Fig. 5 shows the speed and flux waveforms by the proposed programmable LPF. Because the pole of the programmable LPF is located far from the origin, it can be seen that the speed and the flux estimation are stable when the speed is changed. Figure 5(d) shows the time constant of the programmable LPF. The time constant of the programmable LPF varies between 0.0095 and 0.045. Fig. 5(e) shows that the stator flux is exactly estimated.

V. Experimental Results

In order to verify the proposed programmable LPF, the control system is implemented by the software of DSP TMS320C31. The inverter input voltage is $V_{\rm dc} = 300$ [V]. The switching frequency is 5 [kHz]. The current control period is $T_c = 100$ [μs]. Both speed control period and flux control period are $T_s = 1$ [ms]. An encoder of 1024 ppr is mounted on the rotor shaft to monitor the real rotor speed. Load torque is produced by a dynamometer. The stator currents are detected through Hall-type sensors. The stator currents are sampled and held at every sampling instant, then A/D converted with 2 [μs] conversion time. The lower limit of pole a is 1. The motor is 2.2 [kW] three-phase induction motor shown in Table I. The constant k in (9) is 3.

When the motor speed is close to zero, the value of gain compensator in (9) becomes very large. The value is significantly affected by the small detuning of stator resistance. Consequently, the flux control at very low speed close to zero can be unstable. However, the unstability can be avoided by setting the value of synchronous frequency in (9) to 3 [rad/s] by trial and error when the synchronous frequency is lower than 3 [rad/s]. When the synchronous frequency is lower than 3 [rad/s], the synchronous frequency in (9) is set to 3 [rad/s].

The flux control loop acts at a wide speed range (including zero speed). At zero speed, the exact estimation of stator flux is almost impossible since the back emf is zero. When the flux control loop acted at zero speed, the flux control was unstable. The motor speed did not become at a standstill but be fluctuated at very low speed since the d-axis current was fluctuated.

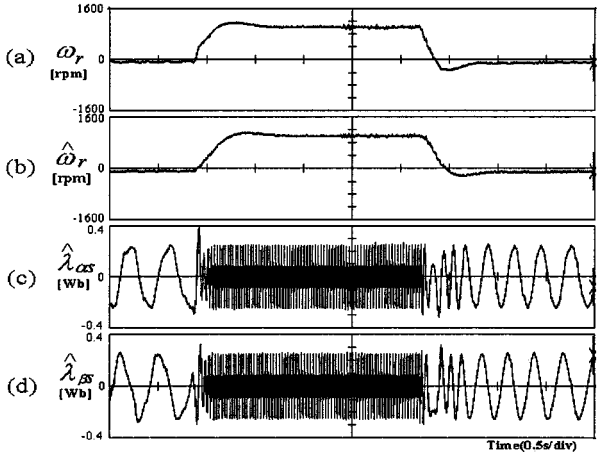

Fig. 6. Speed and flux waveforms by LPF with fixed pole $(s = -20)$ (no load, speed reference (step change): $0 \rightarrow 1000 \rightarrow 0$ [rpm]).

However, the fluctuation was avoided by the use of small stator resistance(about 1.1 [Ω] by trial and error) for the estimation of stator flux (while the measured stator resistance is 1.26 [Ω]) since the d-axis current was not fluctuated. The voltage drop of stator resistance can be negligible as the speed increases because the back emf is high enough. However, if an operation in low speed range is needed, the measured stator resistance should be used.

Fig. 6 shows the speed and the flux waveforms by the LPF with fixed pole $(s = -20)$. Because the LPF does not have the pole close to the origin, the speed and the flux estimation are unstable at the zero speed reference and the speed is not controlled to zero. If the pole is located more far from the origin, the system becomes more unstable.

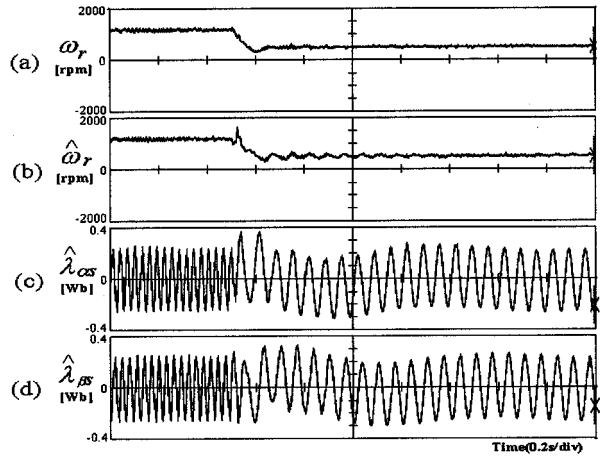

Fig. 7. Step response by LPF with fixed pole $(s = -1)$ (load torque: 4 [N·m], speed reference: $1200 \rightarrow 500$ [rpm]).

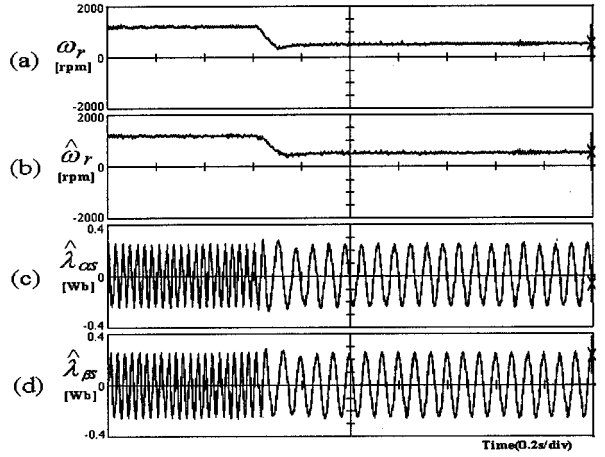

Fig. 8. Step response by programmable LPF (load torque: 4 [N·m], speed reference (step change): $1200 \rightarrow 500$ [rpm]).

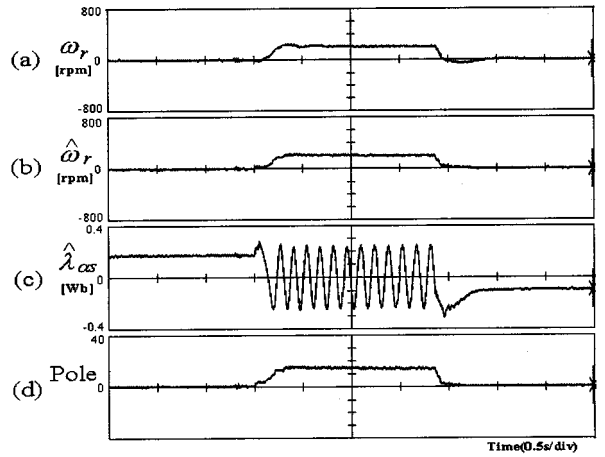

Fig. 9. Speed and flux waveforms by programmable LPF (no load, speed reference (step change): $0 \rightarrow 200 \rightarrow 0$ [rpm]).

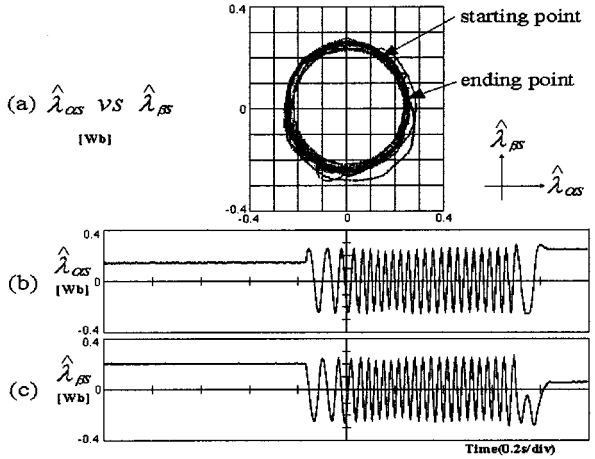

Fig. 10. Flux waveforms by programmable LPF (no load, speed reference (step change): $0 \rightarrow 800 \rightarrow 0$ [rpm]).

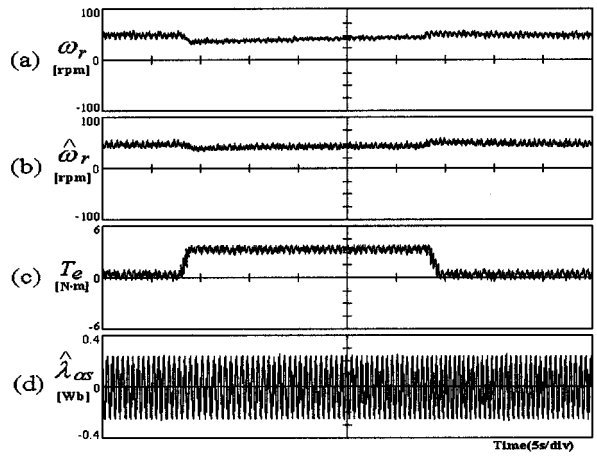

Fig. 11. Speed and torque characteristics by programmable LPF (load torque (step change): 3 [N·m], speed reference: 50 [rpm]).

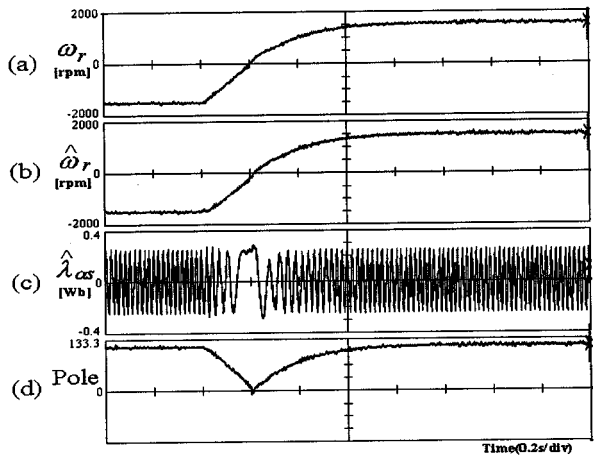

Fig. 12. Speed reversal operation by programmable LPF (no load, speed reference (step change: $-1500 \rightarrow 1500$ [rpm]).

Fig. 7 shows the speed and the flux waveforms by the LPF with fixed pole $(s = -1)$. Because the pole is close to the origin, the flux and the speed estimation are unstable due to the large time constant of the LPF when the speed is changed.

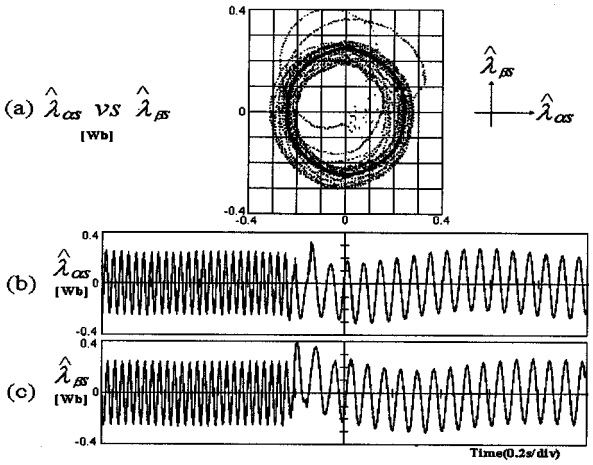

Fig. 13. Locus of stator flux vector by LPF with fixed pole $(s = -1)$ (load torque: 4 [N·m], speed reference (step change): $1000 \rightarrow 500$ [rpm]).

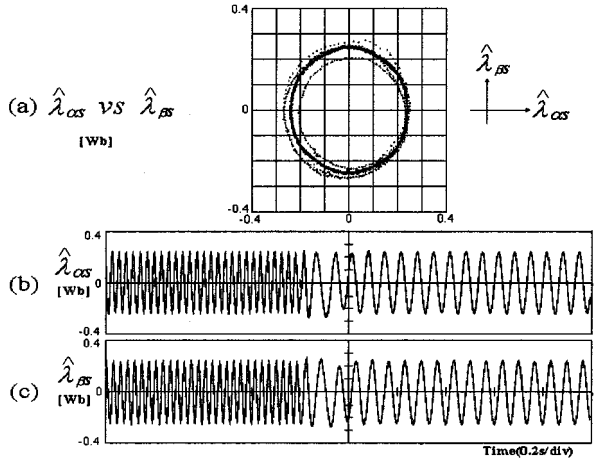

Fig. 14. Locus of stator flux vector by programmable LPF (load torque: 4 [N·m], speed reference (step change): $1000 \rightarrow 500$ [rpm]).

Fig. 8 shows the speed and the flux waveforms by the proposed programmable LPF. It can be seen that because the programmable LPF has the pole farther from the origin, the speed and the flux estimation are stable when the speed is changed.

Figs. 9 and 10 show zero speed start up characteristics by the proposed programmable LPF. The speed and the flux estimation are stable at zero speed compared with Fig. 6. Fig. 9(d) shows that the pole of the programmable LPF varies between 14 and 1(lower limit value of the pole) when the speed is changed.

Fig. 11 shows the speed and torque characteristics by the proposed programmable LPF at low speed. The speed reference is 50 [rpm]. The step load torque (3 [N·m]) is applied, then after about 26 [s], the load is disconnected from the system. Figure 11(a) shows that the speed is decreased by about 20 [rpm] when the load torque is applied to the system, then the speed is converged to the command value. Fig. 11(d) shows that the flux estimation is stable when the load torque is applied and disconnected.

Fig. 12 shows speed reversal characteristics by the proposed programmable LPF. The speed reference is changed from -1500 to 1500 [rpm]. Fig. 12(d) shows that the pole of programmable LPF varies between 104.7 and 1.

Fig. 13 shows the locus of stator flux vector by the LPF with fixed pole $(s = -1)$. The magnitude of the stator flux vector is not constant due to the dc drift.

Fig. 14 shows the locus of the stator flux vector by the programmable LPF. The magnitude of stator flux vector remains nearly constant while the speed is changed.

VI. Conclusion

This paper investigated the drift problem of stator flux estimated by the LPF with fixed pole due to the large time constant of the LPF, and proposed a programmable LPF to solve the drift problem.

The stator flux was exactly estimated by the phase/gain compensator of the proposed programmable LPF in a wide speed range. In addition, the drift problem was much improved by the small time constant of the programmable LPF. Consequently, the speed sensorless drive system with the proposed programmable LPF was able to be more stable than the system with the LPF with fixed pole. The validity of the proposed programmable LPF was proved by simulation and experiments.

References

[1] X. Xu and D. W. Novotny, "Implementation of direct stator flux orientation control on a versatile DSP based system," *IEEE Trans. Ind. Applicat.*, vol. 27, no. 4, pp. 694–700, July/Aug. 1991.

[2] L. Ben-Brahim and A. Kawamura, "A fully digitized field-oriented controlled induction motor drive using only current sensors," *IEEE Trans. Ind. Electron.*, vol. 39, pp. 241–249, June 1992.

[3] G. John, W. Erdman, R. Hudson, C. Fan, and S. Mahajan, "Stator flux estimation from inverter switching states for the field oriented control of induction generators," in *Proc. IEEE IAS Annu. Meet.*, 1995, pp. 182–188.

[4] B. K. Bose and M. G. Simões, "Speed sensorless hybrid vector controlled induction motor drive," in *Proc. IEEE IAS Annu. Meet.*, 1995, pp. 137–143.

[5] B. K. Bose and N. R. Patel, "A programmable cascaded low-pass filter-based flux synthesis for a stator flux-oriented vector-controlled induction motor drive," *IEEE Trans. Ind. Electron.*, vol. 44, no. 1, pp. 140–143, Feb. 1997.

[6] J. Hu and B. Wu, "New integration algorithms for estimating motor flux over a wide speed range," in *Proc. IEEE PESC Rec.*, 1997, pp. 1075–1081.

[7] X. Xu, R. D. Doncker, and D. W. Novotny, "A stator flux oriented induction machine drive," in *Proc. IEEE PESC Rec.*, 1988, pp. 870–876.

[8] T. Ohtani, "Vector control of induction motor without shaft encoder," *IEEE Trans. Ind. Applicat.*, vol. 28, no. 1, pp. 157–164, Jan./Feb. 1992.

[9] H. Tajima and Y. Hori, "Speed sensorless field-orientation control of the induction machine," *IEEE Trans. Ind. Applicat.*, vol. 29, no. 1, pp. 175–180, Jan./Feb. 1993.

[10] T. G. Habetler and D. M. Divan, "Control strategies for direct torque control using discrete pulse modulation," in *Proc. IEEE IAS Annu. Meet.*, Oct. 1989, pp. 514–522.

Myoung-Ho Shin (S'99) was born in Seoul, Korea on November 27, 1967. He received the B.S. and M.S. degrees in electrical engineering from Hanyang University, Seoul, Korea, in 1989 and 1991, respectively, where he is currently pursuing the Ph.D. degree in electrical engineering.

From 1991 to 1996, he was with the Samsung Advanced Institute of Technology (SAIT), Suwon, Korea, as a Senior Researcher. His primary areas of research interest include electrical machines and control systems.

Dong-Seok Hyun (S'79–M'83–SM'91) received the B.E. and M.E. degrees in electrical engineering from Hanyang University, Seoul, Korea, in 1973 and 1978, respectively, and the Ph.D. degree in electrical engineering from Seoul National University, Seoul, Korea, in 1986.

From 1976 to 1979, he was with the Agency of Defense Development, Korea, as a Researcher. He was a Research Associate with the Department of Electrical Engineering, University of Toledo, Toledo, OH, from 1984 to 1985, and a Visiting Professor in the Department of Electrical Engineering, Technical University of Munich, Germany, from 1988 to 1989. Since 1979, he has been with Hanyang University, where he is currently a Professor in the Department of Electrical Engineering and Director of the Advanced Institute of Electrical Engineering and Electronics (AIEE). He is the author of more than 80 publications concerning electric machine design, high-power engineering, power electronics, and motor drives. His research interests include power electronics, digital signal processing, traction, and their control systems.

Dr. Hyun is a member of the IEEE Power Electronics, IEEE Industrial Electronics, IEEE Industry Applications, and IEEE Electron Devices Societies, the Institution of Electrical Engineers (U.K.), the Korea Institute of Electrical Engineers, and the Circuit Control Society.

Soon-Bong Cho was born in Seoul, Korea in 1959. He received the B.S., M.S., and Ph.D. degrees in electrical engineering from Hanyang University in 1983, 1987, and 1997, respectively.

From 1987 to 1991, he was with Hyundai Electrical Engineering Company Research and Development Center, as a Research Engineer. Since 1994, he has been with the Doowon Technical College, Ansung, Korea, where he is an Assistant Professor with the Department of Electrical Engineering. His primary areas of research interest include control systems of electric machines and vector-controlled inverters.

Song-Yul Choe was born in Korea in 1954. He received the Dipl.-Ing. and Ph. D. degrees in electrical engineering from the Technical University of Berlin, Berlin, Germany, in 1986 and 1991, respectively.

From 1986 to 1991, he was with the Technical University of Berlin, as an Assistant Professor. From 1991 to 1993, he joined the Rexroth-Indramat GmbH as a Technical Advisory Member of Research Group for developing motion control systems. Since 1993, he has been working with the Machine Tool Department, Hyundai Precision Co., where he is now the Technical Director. His research interests include Motion Control, Power Conversion Systems, and Computerized Numerical Control.